Section A-Research paper
ISSN 2063-5346

The Role of MHD Casson Nano fluid Flow Over a Nonlinear Inclined Surface with Thermal Radiation, Soret and Dufour Effects in Porous Medium.

Hymavathi Talla[1], N.N.V. Sakuntala[2], K. Fatima[3]

[1,3] Dept. of Applied Mathematics, KRU Dr. MRAR PG centre, Krishna University, Nuzvid, A.P.
[2]Dept. of Science and Humanities (Mathematics), St. Peters Engineering College, Dhulapally, Hyderabad, Telangana.
Corresponding Author: T. Hymavathi

ABSTRACT:

In this paper, we analyze the characteristics of the MHD flow of a Casson Nano fluid over an inclined stretching surface in porous medium under the effects of Soret and Dufour by applying Keller Box method . Non-linear Casson Nano fluid problem is modeled over an inclined surface to extend the occurrence of simultaneous heat and mass transfer by consideringdiverseflow parameters. For a variety of factors, such as the Casson parameter, magnetic parameter, Prandtl number, and suction parameter, numerical analysis and graphing have been done to determine the effects of radiation on velocity and temperature. These profiles of velocity and temperature have been produced. The reported Graphs are contrasted with the current values, which reveal that they are extremely comparable.

Keywords: MHD, Casson Nano fluid, Keller Box, Soret and Dufour effects, Porous medium, inclined surface.

INTRODUCTION:

The fact that many industrially relevant fluids are non-New is crucial to remember here.It is important to keep in mind that many fluids with industrial relevance are non-Newtonian at this point. Because of their importance in petroleum exploration, polymer engineering, various separation processes, food and paper manufacturing, and several other industrial uses, non-Newtonian fluids are now generally acknowledged to be more suitable in actual industrial applications than Newtonian fluids. Diverse models were presented due to these fluids' complexity. The Casson fluid is one of these non-Newtonian models. Casson [1] created the

Casson fluid model first for printing inks and silicone suspension preparations. Over a nano fluid stretching surface, Khan W.A. [2] looked at the production of the steady boundary layer flow, heat transfer, and nano-particle fraction. For the purpose of comparing experimental heat transfer data for nano fluids, Xuan.Y et al. [3] present a novel convective heat transfer correlation. By considering the impact of the interface between solid particles and the base fluid in nano fluids, Xue Q.Z. [4] established a unique model of effective thermal conductivity for nano fluids. An explanation for the aberrant augmentation of convective heat transfer seen in nanofluids was developed by Buongiorno [5]. In this study, Ali. M [6] et al. address the effects of thermal diffusion, diffusion thermo, heat, and mass transfer as well as the characteristics of Casson fluid in mixed convective fluid flow via a moving vertically inclined plate in the presence of a magnetic field. Khan, M. [7] et al. designed a study of the boundary layer heat and mass diffusion (Cattaneo-Christov model) of Jeffery fluid moving across an inclined stretched surface in the presence of a magnetic field. Vijayaragavan R. [8] et al. examined the heat and mass transfer in the unsteady MHD Casson fluid flow past an inclined plate with thermal radiation and heat source/sink. The consequences of heat radiation were also considered by Shamshuddin MD. [9] et al. as they investigated the unsteady magneto hydrodynamic free convection flow of a chemically reacting Casson fluid across an inclined porous plate. Imran Ullah [10] et al. performed numerical simulations to examine how chemical reactions affect the hydro magnetic natural convection flow of Casson nanofluid caused by a nonlinearly stretching sheet immersed in a porous medium under the influence of thermal radiation and convective boundary conditions. Thermophoresis and Soret-Dufour effects on magneto hydrodynamic mixed convective heat and mass transport over an inclined flat plate with a non-uniform heat source/sink were the main topics of study for Dulal Pal [11] et al. M.M. Bhatti [12] et al. look into the impact of magneto hydrodynamics on entropy generation on the peristaltic blood flow of the Casson fluid model. The effects of thermal diffusion and diffusion thermo effects, as well as the parameters of heat and mass transfer of Casson fluid in mixed convective fluid flow via a moving vertically inclined plate in the presence of a magnetic field, are examined by Ali Mujeeb [13] et al. C.S.K. Raju [14] et al. investigated the effects of magneto hydrodynamic mixed convective heat and mass transfer over an inclined flat plate with a non-uniform heat source/sink on three-dimensional magneto hydrodynamic nanofluid flow over a nonlinearly permeable stretched sheet in relation to spatial and temperature dependent heat generation or absorption.

Govindarajan [15] investigated nanofluid flow over a tilted sheet by including a non-

uniform temperature. The transmission of mass and heat was depicted in Khan et al.'s [16] picture of MHD Jeffery nanofluid flow across an inclined sheet. On a slanted surface, Chakraborty [17] studied nanofluid flow with radiation effects. The effects of a Casson Nanofluid boundary layer flow across an inclined extended surface are examined by Khuram Rafique [18] et al. with the aid of Soret and Dufour. Hymavathi [19] et al. looked at the Soret and Dufour effects on a viscous fluid that was undergoing chemical reaction while flowing through a moving vertical plate. In order to characterize the behaviour of non-Newtonian fluids, Hymavathi [20] et al. analyze the Casson fluid model by looking at the diffusion of chemically reactive species of a non-Newtonian fluid towards an exponentially increasing surface. Hymavathi [21] et al. used the Homotopy Analysis Method to study the impact of radiation and chemical reaction on the flow of an electrically conducting visco-elastic fluid through an exponential stretching sheet via a porous medium.

MATHEMATICAL FORMULATION:

$$\frac{\partial u}{\partial x}+\frac{\partial v}{\partial y}=0 \tag{1}$$

$$u\frac{\partial u}{\partial x}+v\frac{\partial u}{\partial y}=\upsilon(1+\frac{1}{\beta})\frac{\partial^2 u}{\partial y^2}+[\beta_t(T-T_\infty)+\beta_c(C-C_\infty)]g\cos\gamma-\frac{\upsilon}{k'}u-\frac{\sigma {B_0}^2(x)u}{\rho} \tag{2}$$

$$\boldsymbol{u}\frac{\partial \boldsymbol{T}}{\partial \boldsymbol{x}}+\boldsymbol{v}\frac{\partial \boldsymbol{T}}{\partial \boldsymbol{y}}=\alpha\frac{\partial^2 \boldsymbol{T}}{\partial \boldsymbol{y}^2}-\frac{1}{(\delta \boldsymbol{c})_f}\frac{\partial \boldsymbol{q_r}}{\partial \boldsymbol{y}}+\tau\left[\boldsymbol{D_B}\frac{\partial \boldsymbol{C}}{\partial \boldsymbol{y}}\frac{\partial \boldsymbol{T}}{\partial \boldsymbol{y}}+\frac{\boldsymbol{D_T}}{\boldsymbol{T_\infty}}\left(\frac{\partial \boldsymbol{T}}{\partial \boldsymbol{y}}\right)^2\right]+\frac{\boldsymbol{D_T K_T}}{\boldsymbol{C_s C_p}}\frac{\partial^2 \boldsymbol{C}}{\partial \boldsymbol{y}^2} \tag{3}$$

$$\boldsymbol{u}\frac{\partial \boldsymbol{C}}{\partial \boldsymbol{x}}+\boldsymbol{v}\frac{\partial \boldsymbol{C}}{\partial \boldsymbol{y}}=\boldsymbol{D_B}\frac{\partial^2 \boldsymbol{C}}{\partial \boldsymbol{y}^2}+\frac{\boldsymbol{D_T K_T}}{\boldsymbol{T_\infty}}\frac{\partial^2 \boldsymbol{T}}{\partial \boldsymbol{y}^2} \tag{4}$$

where $q_r=-\frac{4\sigma^*}{3k^*}\frac{\partial T^4}{\partial y}$ the Rosseland approximation (for radiation flux) (5)

Where σ^* is the Stefan-Boltzmann constant and $\boldsymbol{k}^*$ is the mean absorption coefficient. It is assumed that the temperature difference between the free steam T∞ and local temperature T is small enough, expanding T4 in Taylor series about T∞ and neglecting higher order terms for:

$$\boldsymbol{T}^4\cong 4\boldsymbol{T}_\infty^3\boldsymbol{T}-3\boldsymbol{T}_\infty^4 \tag{6}$$

With the equations (5) and (6) equation (3) reduced into

$$u\frac{\partial T}{\partial x}+v\frac{\partial T}{\partial y}=\left[\alpha+\frac{16\sigma^{*}}{3k^{*}(\delta c)_{f}}\right]\frac{\partial^{2}T}{\partial y^{2}}+\tau\left[D_{B}\frac{\partial c}{\partial y}\frac{\partial T}{\partial y}+\frac{D_{T}}{T_{\infty}}\left(\frac{\partial T}{\partial y}\right)^{2}\right]+\frac{D_{T}K_{T}}{C_{s}C_{p}}\frac{\partial^{2}C}{\partial y^{2}} \quad (7)$$

Where u and v are the velocity components in the x and y directions, respectively,
g - acceleration due to gravity,
k' - permeable coefficient of porous medium,
B_0 - uniform magnetic field strength,
σ - electrical conductivity,
υ - viscosity,
δ_f - density of the base fluid,
δ_p - density of the nano particle,
β - Casson parameter,
β_T - coefficient of thermal expansion,
β_C - coefficient of concentration expansion,
D_B - Brownian diffusion coefficient and
D_T - thermophoresis diffusion coefficient,
k - thermal conductivity,
$(\delta c)_p$ is the heat capacitance of the nano particles,
$(\delta c)_f$ is the heat capacitance of the base fluid,
$\alpha=\frac{k}{(\delta c)_f}$ is the thermal diffusivity parameter,
$\tau=\frac{(\delta c)_p}{(\delta c)_f}$ is the ratio between the effective heat capacity of the nano particle and heat capacity of the fluid.
Boundary conditions are :

$$\begin{aligned} &u=U_w(x)=ax^m,\ v=0,\ T=T_w\ \ C=C_w && at\ y=0\\ &u\to U_\infty(x)=0,\ v\to 0,\ T\to T_\infty,\ C\to C_\infty && as\ y\to\infty \end{aligned} \quad (8)$$

In order to create non-linear ordinary differential equations, the non-linear partial differential equations are reduced. For that purpose, the stream function $\psi=\psi(x,y)$ is defined as:

$$u=\frac{\partial\psi}{\partial y},\ v=-\frac{\partial\psi}{\partial x}, \quad (9)$$

The momentum energy and concentration equations can be transformed into the corresponding ordinary differential equations by introducing the similarity transformations

$$\eta = y\sqrt{\frac{(m+1)ax^{m-1}}{2\upsilon}}\ ,\ \psi(x,y) = \sqrt{\frac{2\upsilon ax^{m+1}}{m+1}}\, f(x,\eta),\ \ \theta(\eta) = \frac{T - T_\infty}{T_w - T_\infty}\ ,\ \phi(\eta) = \frac{C - C_\infty}{C_w - C_\infty} \qquad (10)$$

Where η is the similarity variable and f is the dimensionless stream function considering $f(x,\eta) = f(\eta)$.

The momentum, energy and concentration equations are transformed to

$$(1+\frac{1}{\beta})f''' - \left(\frac{2m}{m+1}\right)f'^2 + ff'' + \left(\frac{2}{m+1}\right)(\lambda\theta - \delta\phi)\cos\gamma - \frac{\upsilon}{k^*}u - \left(\frac{2}{m+1}\right)(M+k_1)f' = 0 \qquad (11)$$

$$\mathrm{Pr}_N\,\theta'' + f\theta' + N_b\phi'\theta' + N_t\theta'^2 + D_f\phi'' = 0 \qquad (12)$$

$$\phi'' + Le\ f\phi' + Sr\ Le\,\theta'' = 0 \qquad (13)$$

With the boundary conditions

$$\begin{array}{lllll} f=0, & f'=1, & \theta=1 & \phi=1 & at\ \eta=0 \\ f'=0, & f''=0 & \theta=0 & \phi=0 & as\ \eta\to\infty \end{array} \qquad (14)$$

Where

$$\lambda = \frac{Gr_x}{\mathrm{Re}},\ \ \delta = \frac{Gc}{\mathrm{Re}},\ \ M = \frac{\sigma B_0^2(x)}{a\rho},\ \ Le = \frac{\upsilon}{D_B},\ \mathrm{Pr} = \frac{\upsilon}{\alpha},\ \ N_b = \frac{\tau D_B(C_w - C_\infty)}{\upsilon},\ \mathrm{Re} = \frac{u_w x}{\upsilon}\ ,$$

$$N_t = \frac{\tau D_t(T_w - T_\infty)}{\upsilon T_\infty},\ Gr_x = \frac{g\beta_t(T_w - T_\infty)x}{a\upsilon_\infty},\ \ Gc_x = \frac{g\beta_c(C_w - C_\infty)x}{a\upsilon},\ \mathrm{Pr}_N = \frac{1}{\mathrm{Pr}}(1+\frac{4}{3}N),$$

$$N = \frac{4\sigma^* T^3{}_\infty}{\alpha k^*},\ \ D_f = \frac{D_T K_T(C_w - C_\infty)}{\upsilon C_s C_p(T_w - T_\infty)},\ \ Sr = \frac{D_T K_T(T_w - T_\infty)}{\upsilon T_\infty(C_w - C_\infty)},\ \mathrm{k}_1 = \frac{\upsilon}{k'a} \qquad (15)$$

Here, primes denote the differentiation with respect to η,

λ Buoyancy parameter,

δ Solutal buoyancy parameter,

M is the magnetic parameter called Hartmann number,

Pr denotes the Prandtl number,

Le denotes the Lewis number,

Nb denotes the Brownian motion parameter,

Nt indicates thermophoresis parameter, and

N is the radiation parameter.

RESULTS AND DISCUSSION:

The converted non-linear differential equations ((8) and (9) with boundary conditions (10), which comprise the finite-differences approach, Newton's scheme, and block elimination method, are often explained using a finite difference scheme known as the Keller box method. Using MATLAB, velocity and temperature profiles are visually shown for a range of values of variables, including Casson, Magnetic, buoyancy, thermo-poresis, radiation parmeter effects, and Prandtl numbers. The Keller Box approach yields numerical solutions.

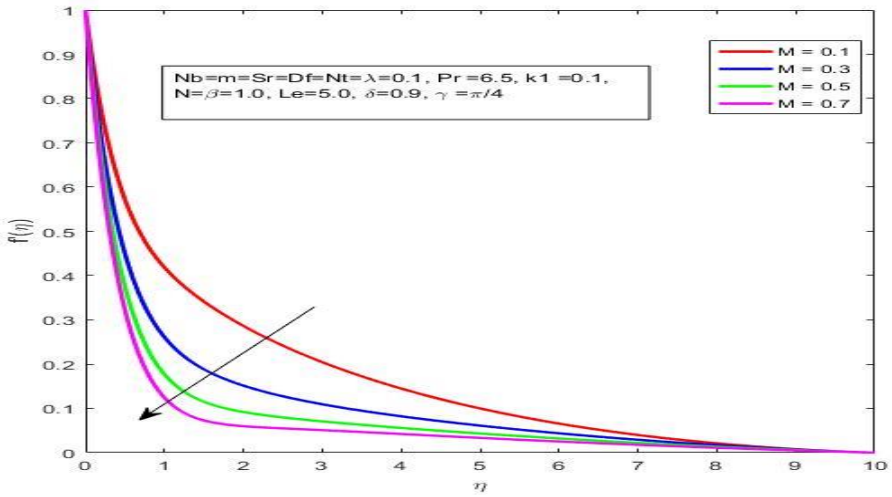

Graph-1 : Velocity Profiles with diverse values of M

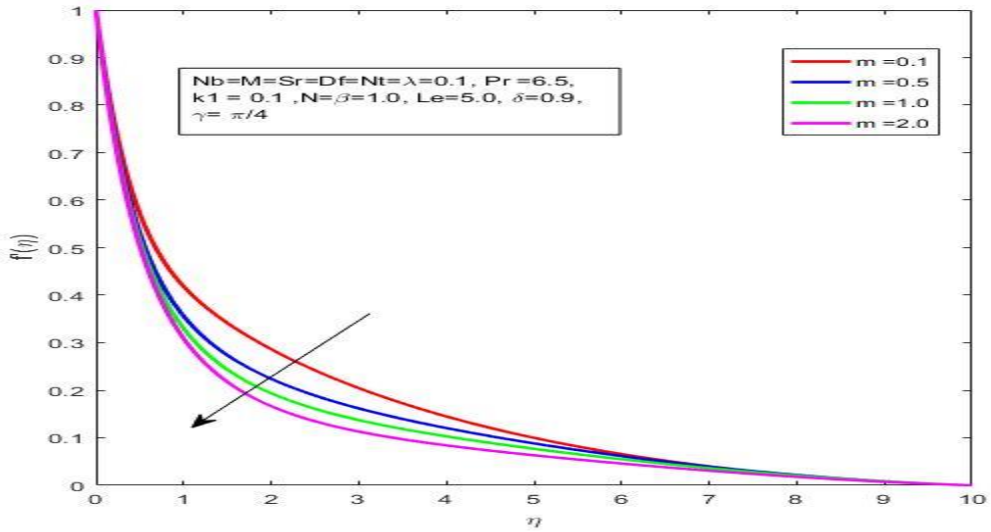

Graph-2 : Velocity Profiles with diverse values of m

Graph 1 is an illustration of how factor M affects the velocity profile. The velocity outline decreases, as seen in Graph 1, when the constraint M is strengthened. By reducing the liquid's speed, the magnetic field creates the Lorentz force. On the other hand, with large values of the non-linear stretching parameter m, as shown in Graph 2, the velocity profile slows down. physically, as m rises, the boundary layer's thickness gets thinner.

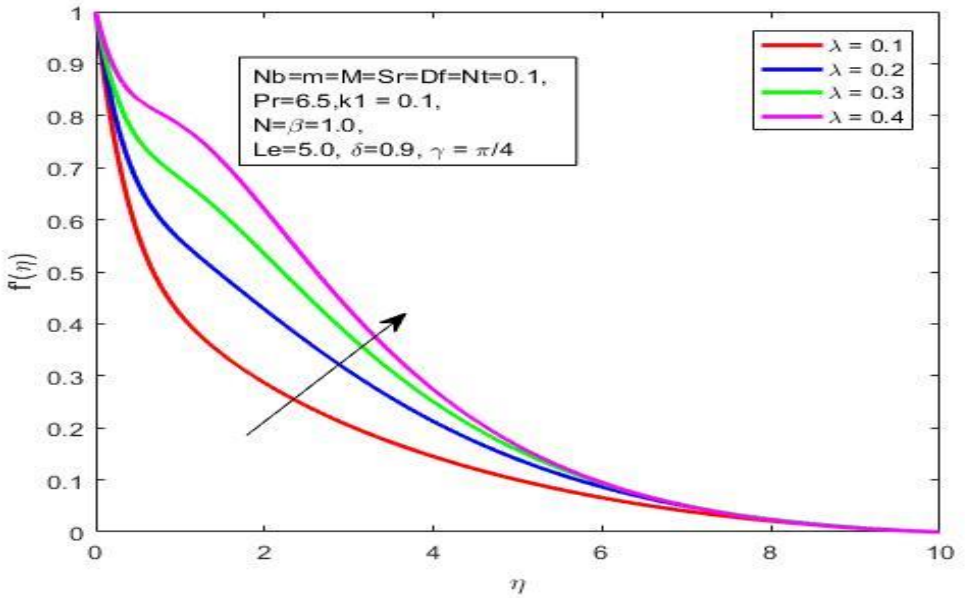

Graph-3 : Velocity Profiles with diverse values of λ.

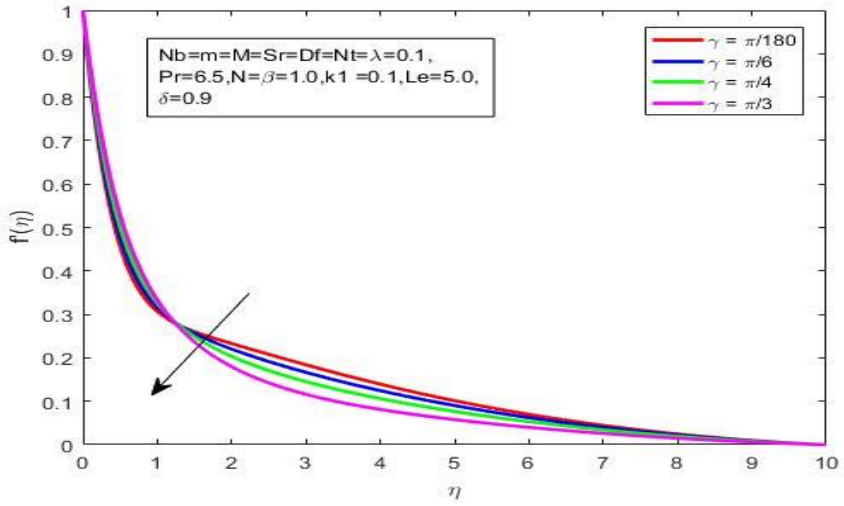

Graph-4 : Velocity Profiles with diverse values of γ.

The impact of the buoyancy factor is illustrated in Graph 3. The velocity profile has been seen to grow as the buoyancy limit λ is raised. That's why the boundary layer thickness and velocity are increasing, as the buoyancy effect intensifies the fluid flow.

Interpretation of inclination factor γ on velocity is shown in Graph 4, it appears that by increasing the values of γ, the velocity decreases. Furthermore, the facts show that the vertical state of the sheet at γ= 0 will exert the strongest gravitational pull on flow. However, the sheet will be different if $\gamma = 90^0$.

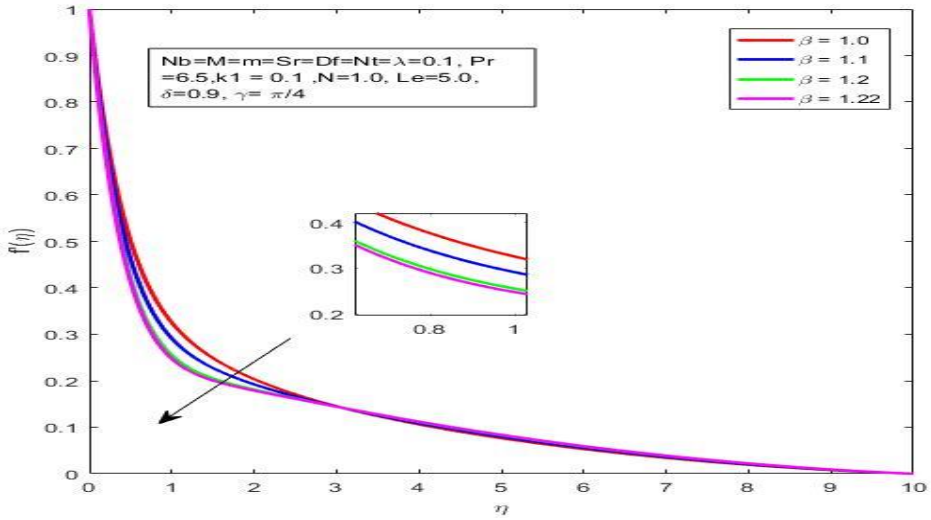

Graph-5 : Velocity Profiles with diverse values of β.

The effect of the Casson parameter β on the velocity parameter is depicted in Graph 5. High values of the Casson parameter are observed to cause the velocity profile to decrease. This behaviour results from the Casson parameter's ability to reduce yield stress by raising fluid viscosity. As a result, the momentum boundary layer's thickness reduces. The velocity shape grows as the solutal buoyancy component δ increases, as shown in Graph 6. Physically, the buoyancy parameter δ causes an increase in velocity by reducing the forces of viscosity.

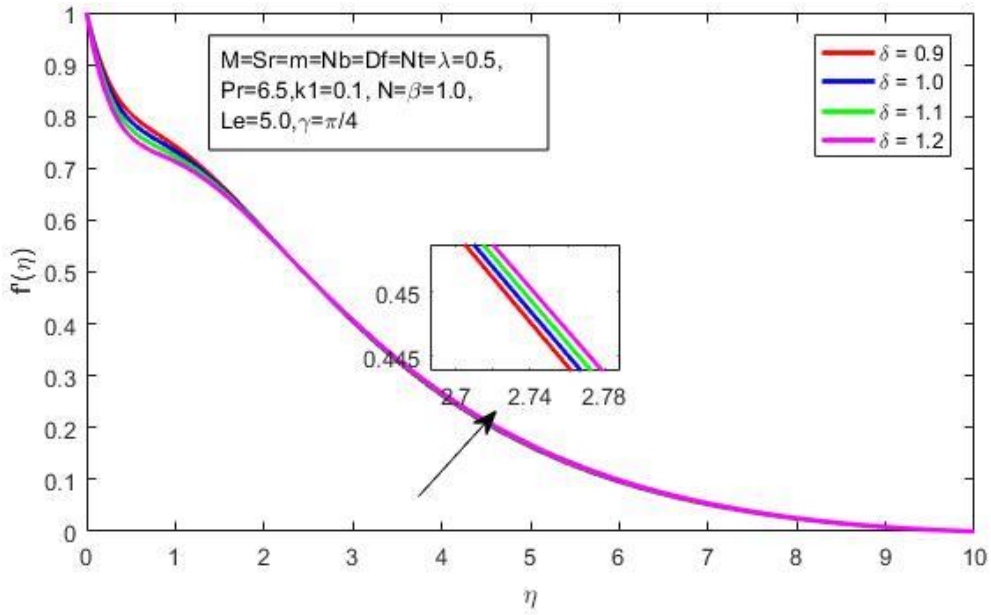

Graph-6 : Velocity Profiles with diverse values of δ.

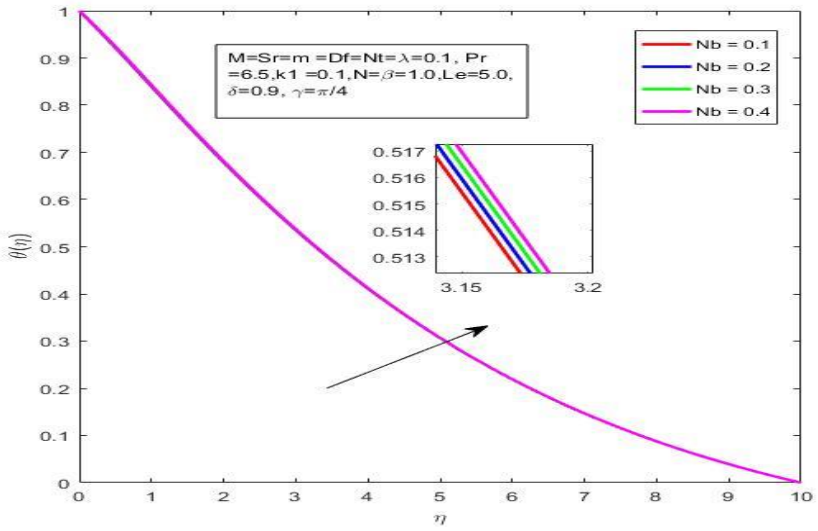

Graph-7 : Temperature Profiles for diverse values of Nb.

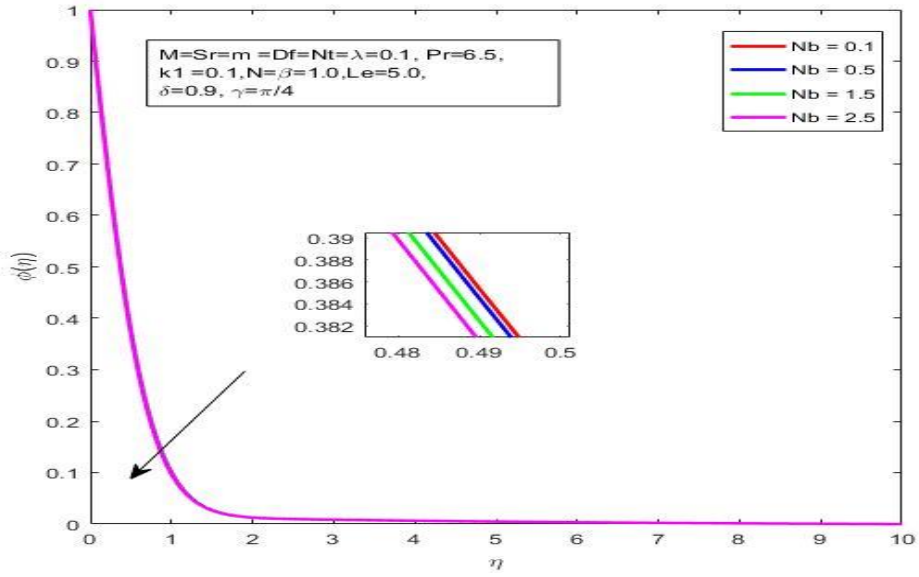

Graph-8 : Concentration Profiles with diverse values of Nb.

Graphs 7 and 8 show, respectively, how Brownian motion affects temperature & concentration profiles. When Nb is enlarged, the temperature sketch expands, but the concentration distribution glows in a different way.

The boundary layer is physically heated by the Brownian motion that is prone to transport nano particles from the expanding sheet to the stationary liquid. Thus, there is a decrease in nano particle absorption.

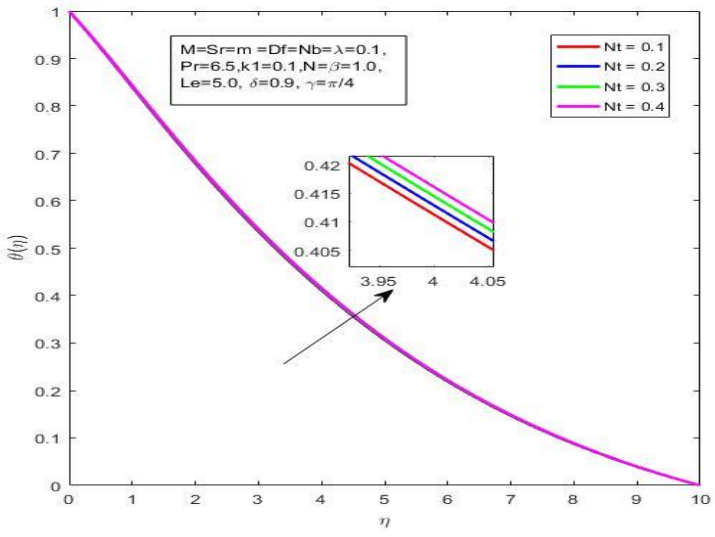

Graph-9 : Temperature Profiles with diverse values of Nt.

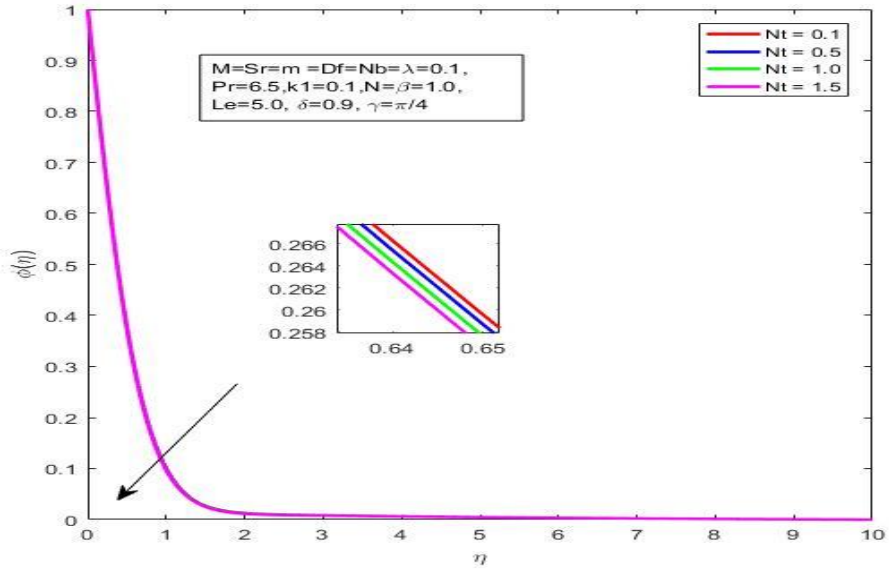

Graph-10 : Concentration Profiles for diverse values of Nt.

Graphs 9 and 10 display the temperature & concentration profiles for modified thermo-phoresis parameter Nt values. Because thermo-phoresis forces tiny particles to move from a warmish surface to a cold one, it is believed that increasing the thermo-phoresis parameter Nt raises temperature and lowers the concentration contours.

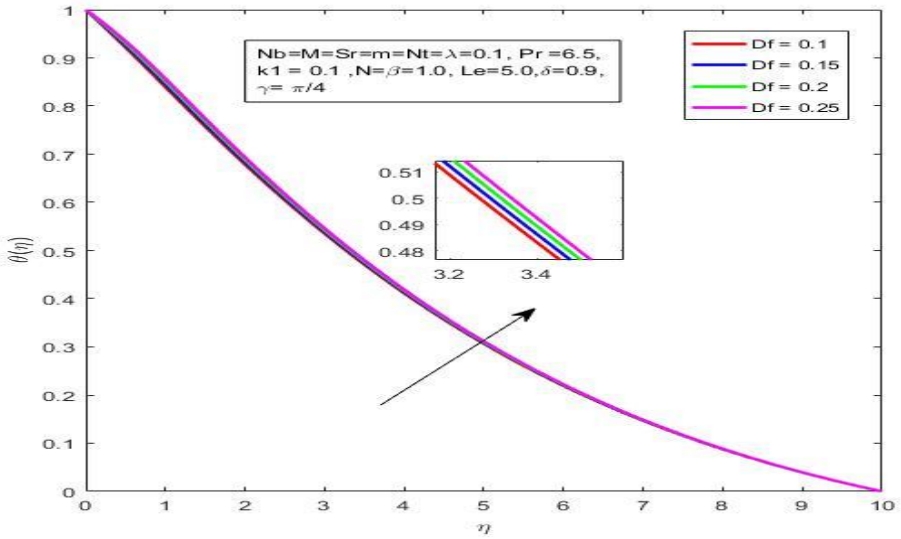

Graph-11 : Temperature Profiles with diverse values of Df.

Temperature profile is shown to rise as the parameter Df is increased in Graph 11. This can be explained by a rise in the Dufour parameter, which causes a rise in the gradient of concentration and a rise in the mass diffusion rate. As a result, the rate of energy transfer related to the particles rises. As a result, the temperature profiles are getting better.

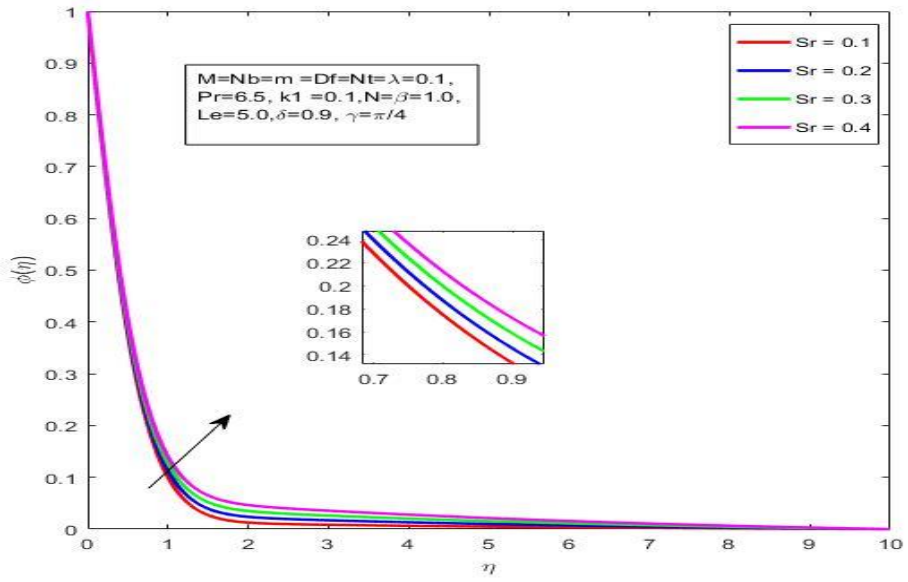

Graph-12 :

Concentration Profiles with diverse values of Sr.

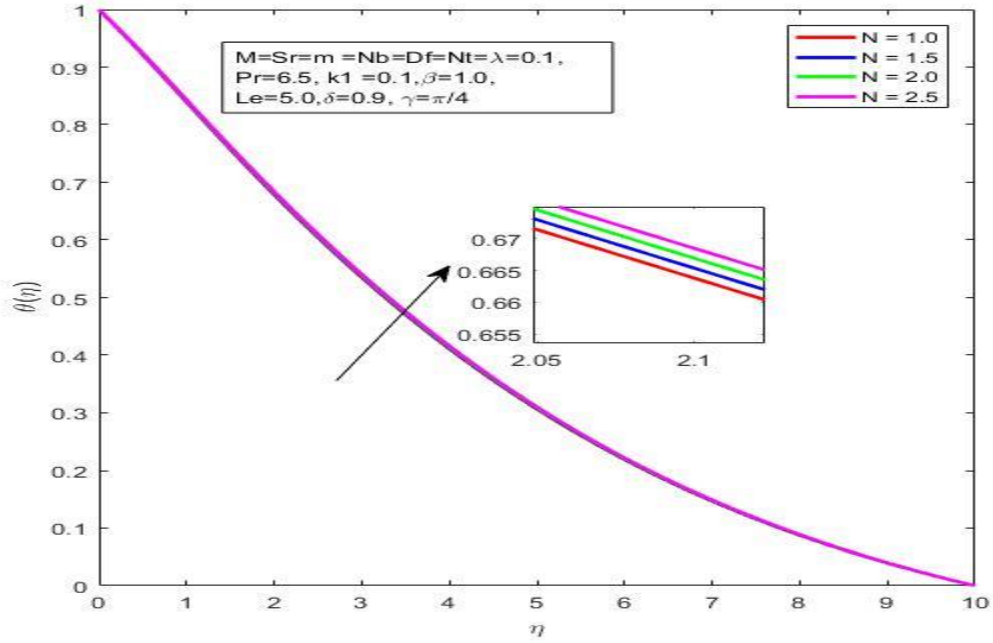

Graph-13: Temperature Profiles with diverse values of N.

Similar to how the Dufour number affects the temperature profile, the Soret number has an effect on the concentration profile. The concentration profile rises as parameter Sr rises, as shown in Graph 12. Graph 13 also shows a temperature profile that is improved for high amounts of N.

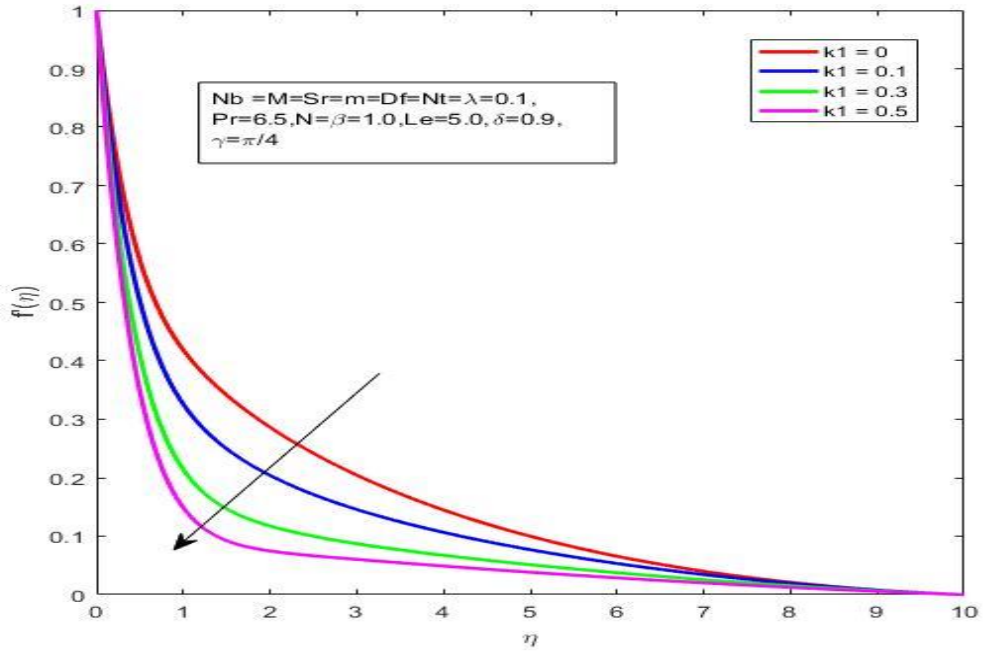

Graph-14 : Velocity Profiles with diverse values of k_1.

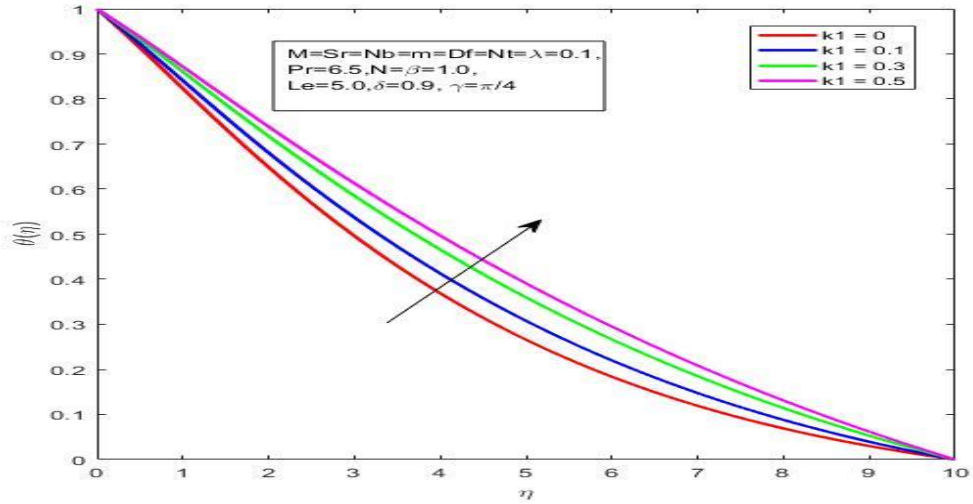

Graph-15 : Temperature Profiles with diverse values of k_1.

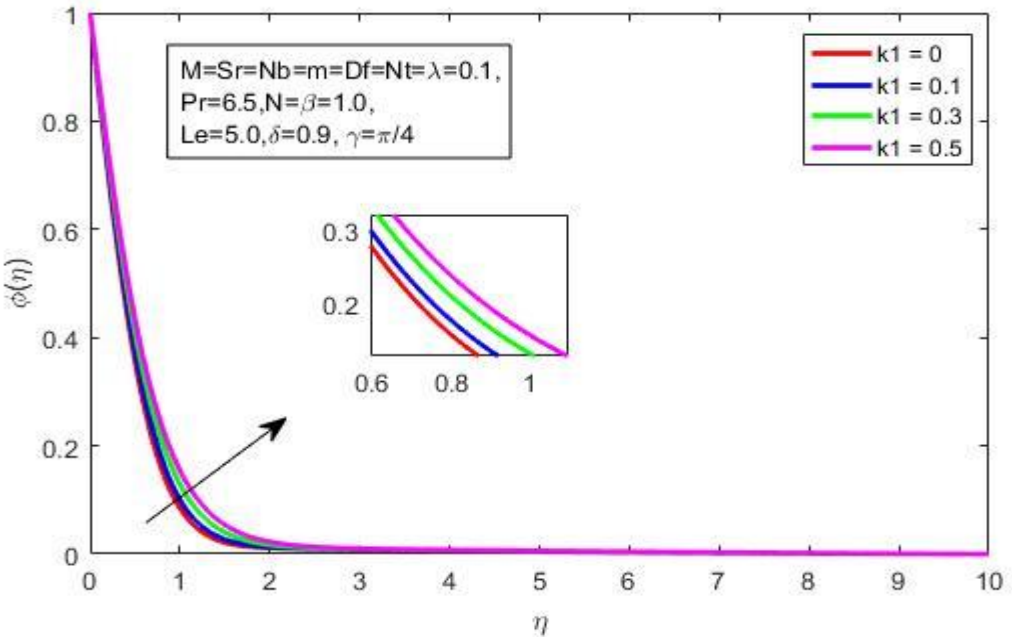

Graph-16: Concentration Profiles with diverse values of k_1.

Influence of porosity parameter k_1 on velocity, temperature, concentration profiles is shown in Graph-14. Graph-15, Graph-16. According to the graph, raising the porosity parameter (k_1) decreases velocity while increasing temperature and concentration.

CONCLUSIONS:

The key conclusions of current study are

1. As Casson fluid factor rises, so does velocity profile.

2. When the buoyancy and solutal buoyancy parameters are modified, the velocity profile improves.

3. As the radiation factor is increased, the temperature profile rises.

4. Increase in inclination parameter occurs a drop in velocity outline.

5. Enhancement in the temperature profile is due to the Dufour effect.

6. Mass diffusion and fluid energy increase by boosting the Brownian motion factor.

7. The profile of temperature is elevated by thermophoresis factor, while concentration is lowered.

8. The parameters such as porous and visco-elastic have the effect of increasing the heat & mass transfer rate of the region of boundary layer.

REFERENCES:

[1] N Casson. A Flow Equation for Pigment-Oil Suspensions of the Printing Ink Type. Pergamon Press, Oxford 1959, p. 84-104.

[2] Khan WA, Pop I. Boundary-layer flow of a nano fluid past a stretching sheet. *Int J Heat and Mass Trans. 53:2477–83, (2010).*

[3] Xuan Y, Li Q, Investigation on convective heat transfer and flow features of nano fluids, Journal of Heat Transfer 125:151-155, (2003).

[4] Xue Q-Z, Model for effective thermal conductivity of nano fluids, Physics Letters A 307:313–317, (2003).

[5] Buongiorno J., Convective transport in nano fluids, *Journal of Heat Transfer, 128(3):240–50, (2006).*

[6] Ali M, Aruna G, Raju RS. MHD boundary layer casson fluid flow over avertically inclined plate: grid study and convergence analysis of finite element technique. *Journal of Nano fluids, 7(6):1195–207. (2018).*

[7] Khan M, Shahid A, Malik MY, Salahuddin. T, Thermal and concentration diffusion in Jeffery nano fluid flow over an inclined stretching sheet: a generalized Fourier's and Fick's perspective, *Journal of Molecular Liquids, 251:7–14, (2018).*

[8] Vijayaragavan R, Kavitha M.A., Heat and mass transfer in unsteady MHD casson fluid flow past an inclined plate with thermal radiation and heat source/sink. *Research Journal of Engineering and Technology, 9(2), 214–33, (2018).*

[9] Shamshuddin MD, Mishra SR, Thumma T., Chemically reacting radiative casson fluid over an inclined porous plate: a numerical study, *Numerical Heat Transfer and Fluid Flow, Springer, 469–479, (2019).*

[10] Ullah I, Khan I, Shafie S. MHD natural convection flow of Casson nano fluid over non linearly stretching sheet through porous medium with chemical reaction and thermal radiation. Nanoscale Research Letters, 11:527, (2016).

[11] Pal D, Mondal H. Influence of Soret-Dufour and thermophoresis on hydro magnetic mixed

convection heat and mass transfer over an inclined flat plate with non-uniform heat source/sink and chemical reaction. Int J Comput Methods Eng Sci Mech. (2018) 19:49–60.

[12] Bhatti M.M, Abbas, M.A, Rashidi M.M, Entropy generation for peristaltic blood flow with casson model and consideration of magneto hydrodynamics effects, *Walailak Journal of Science and Technology, 14:451–61, (2016).* .

[13] Ali M, Aruna G, Raju RS. MHD boundary layer casson fluid flow over a vertically inclined plate: grid study and convergence analysis of finite element technique, *Journal of Nano fluids, 7:1195–207, (2018).*

[14] Raju C.S.K, Sandeep N, Babu M.J, Sugunamma.V, Dual solutions for three dimensional MHD flow of a nanofluid over a nonlinearly permeable stretching sheet, Alexandria Eng J 55:151–162, (2016).

[15] Govindarajan A. Radiative fluid flow of a nanofluid over an inclined plate with non-uniform surface temperature. J Phys Conf. 1000:012173, (2018).

[16] Khan M, Shahid A, Malik MY, Salahuddin T. Thermal and concentration diffusion in Jeffery nanofluid flow over an inclined stretching sheet: a generalized Fourier's and Fick's perspective. J Mol Liquids. 251:7–14, (2018).

[17] Chakraborty T, Das K, Kundu PK. Ag-water nanofluid flow over an inclined porous plate embedded in a non-Darcy porous medium due to solar radiation. J Mech Sci Technol. 31:2443–9, (2017).

[18] Khuram Rafique, Muhammad Imran Anwar, Masnita Misiran, Ilyas Khan, S. O. Alharbi , Phatiphat Thounthong and K. S. Nisar, Numerical Solution of Casson Nano fluid Flow Over a Non-linear Inclined Surface With Soret and Dufour Effects by Keller-Box Method, Frontier's in Physics, 7:139, (2019).

[19] Hymavathi Talla, P. Vijaykumar and B. Akkaya, Homotopy Analysis to Soret and Dufour Effects of Heat and Mass Transfer of Chemically Reacting Fluid past a Moving Vertical Plate with Viscous Dissipation, *IOSR Journal of Mathematics, 11 (6), 106-121 (2015).*

[20] Hymavathi Talla and W. Sridhar, Numerical solution to Diffusion of Chemically Reactive Species of a Casson Fluid Flow over an Exponentially Stretching Surface, International Journal of Chemical Engineering Research, 9 (2), 207-221 (2017).

[21] Hymavathi Talla and N.N.V. Sakuntala, Effect of radiation and chemical reaction on heat

and mass transfer of MHD visco-elastic fluid flow over an exponentially stretching sheet through porous medium, *International Journal of Mechanical Engineering and Technology, 10 (9), 46-58, (2019).*